Biochimica et Biophysica Acta, 1024 (1990) 271–277
Elsevier

BBAMEM 74845

Temperature- and concentration-dependence of urea permeability of human erythrocytes determined by NMR

Daniel M. Karan and Robert I. Macey

Division of Cell Physiology and Biophysics, Department of Molecular and Cellular Biology, University of California, Berkeley, CA (U.S.A.)

(Received 11 December 1989)

Key words: Urea; Membrane permeability; Erythrocyte; NMR; (Temperature dependence)

The temperature- and concentration-dependence of [^{13}C]urea self-exchange across the human red cell membrane has been determined by NMR measurements of T_1 (spin-lattice) relaxation times. T_1 for intracellular label is 17 s, which is much longer than the urea exchange time across the cell membrane (about 0.5 s). T_1 for urea in extracellular solution is quenched with 17 mM of impermeable Mn^{2+} in less than 2 ms. Hence the observed T_1 (corrected for intracellular decay) is a measure of urea exchange across the cell membrane. The method is tested by showing both PCMBS and increasing concentrations of urea lengthen T_1. Urea exchange permeability, defined as $P_{urea} = flux/conc$, can be described by $P_{urea} = V_{max}/(K_{1/2} + conc)$. Studies of temperature-dependence showed that activation energies were strongly dependent on both temperature and concentration. However, this apparently anomalous behavior was resolved into two well-behaved functions, $K_{1/2}$ and V_{max}, with linear Arrhenius plots and apparent 'activation energies' of 15.5 and 12.4 kcal/mol, respectively. These were used to construct an equation for calculating P_{urea} at any concentration and temperature. Assuming a simple channel model with single binding, $K_{1/2}$ becomes the dissociation equilibrium constant for the site with $\Delta H^\circ = 15.5$ kcal/mol and $\Delta S^\circ = 51.8$ cal/(mol · deg); dissociation is entropically driven.

Introduction

The permeability of urea in the human red cell is orders of magnitude greater than permeabilities reported for lipid bilayers [1–6]; it shows saturation at high urea concentrations and it is inhibited by analogs of urea [1,2]. These are the essential characteristics of a facilitated transport system. Physiologically, facilitated urea transport is essential to minimize the severe volume perturbations that would be experienced by any red cell circulating through the renal medulla. Further, red cells with defective urea transport systems will function as urea traps; they will carry concentrated urea out of the medulla and impair the counter-current concentrating mechanism [8]. Finally, urea transport plays a key role in sickle cell anemia because it inhibits hemoglobin polymerization [9]. When red cells enter the renal medulla of a sickle cell (disease or trait) subject, the rapid influx of high concentrations of urea helps ameliorate the severe cell dehydration, hypoxia and acidosis inflicted by the local environment.

A full appreciation of the mechanism of urea transport, as well as its physiological role, requires accurate estimates of parameters that characterize its kinetics. Current interpretations are ambiguous because there is no general agreement on the magnitudes of these quantities, nor is there general agreement on the appropriate kinetic model. Depending on the urea concentration, the time constants for exchange vary between 0.1 to 5 s. This rapid exchange has necessitated use of continuous flow-filtration methods for measurements of parameters. Unfortunately, continuous flow systems have a restricted range of rates that they can resolve. The lower bound is limited by problems of maintaining turbulent mixing throughout the length of the tube. Further problems may arise in obtaining a representative sample from a filtration port located at the periphery of the tube. Detailed exchange studies have been reported in only two instances [1,2] and the values reported for exchange parameters in these two articles show substantial disagreement. Other ambiguities also become apparent upon comparison of various estimates of the temperature-dependence of urea transport [1,10].

Abbreviation: PCMBS, *para*-chloromercuribenzene sulfonate.

Correspondence: R.I. Macey, Department of Molecular and Cellular Biology, University of California, Berkeley, CA 94720, U.S.A.

In this paper we introduce an independent ^{13}C-labelled urea NMR method to measure the parameters of urea equilibrium exchange. This method, an application of the technique introduced by Conlon and Outhred [11] for measurements of water permeability, does not appear to suffer from the same limitations as continuous flow-filtration or as light-scattering measurements of cell volume perturbations. It readily adapts to measurements of activation energies, and our results show that the apparently anomalous temperature-dependence of urea transport is easily resolved into the 'well behaved' temperature-dependence of the exchange transport parameters V_{max} and $K_{1/2}$

Methods

Sample preparation

Freshly drawn venous blood (with EDTA anticoagulant) obtained from donors was used for NMR experiments within 24 h of collection. Just prior to an experiment, the blood was washed several times in either 150 mM NaCl or in a solution containing 135 mM KCl and 15 mM NaCl. Cells to be used immediately were left as a packed pellet and cells to be used within a few hours were resuspended in the wash solution. [^{13}C]Urea was obtained from MSD Isotopes or Isotec. D_2O was obtained from Sigma.

Typically, 1 ml samples in 5-mm Wilmad tubes were run on a Bruker AM300 spectrometer. Samples in various [^{13}C]urea concentrations were prepared from stock solutions containing [^{13}C]urea, NaCl and/or KCl, in pure H_2O or D_2O/H_2O mixtures. Stock solutions were as follows: the isotonic salt solution (referred to as KN) contained 135 mM KCl and 15 mM NaCl in H_2O or D_2O; Two urea stock solutions were used to provide all concentrations of interest, 434 mM [^{13}C]urea (in KN) and 2170 mM urea containing 434 mM [^{13}C]urea and 1736 mM [^{12}C]urea (in KN). To make, for example, a 1 ml sample at 500 mM urea, the following were combined: 0.15 ml of 2170 mM urea-stock, 0.25 ml of 434 mM urea-stock, 0.1 ml of KN-stock, 0.1 ml of 100 mM $MnCl_2$ and 0.4 ml of packed pellet. This provided our standard 17 mM Mn^{2+} in the external medium for signal quenching and a final equilibrium urea concentration of 500 mM. The final hematocrit of all samples measured was 38–40% and was high enough to provide self buffering (no external buffer was utilized). The pH of the cell suspension in both 100 mM and 1000 mM urea was measured by glass electrode under experimental conditions with isotonic 50/50 (H_2O/D_2O) as well as pure H_2O. The measured pH in all cases was in the range 7.44 to 7.49.

Cells for the PCMBS experiments were prepared in essentially the same manner as for the concentration-temperature studies with the following exceptions. Cells were incubated at room temp. for 1.5 h at a hematocrit of 4% in 0.05 mM PCMBS solution containing 27 mM Sucrose, 122 mM KCl and 14 mM NaCl. The cells were then centrifuged and the packed pellet was used as above.

Chemicals

All chemicals were reagent grade with the exception of urea and 99.8% D_2O (Sigma) [^{12}C]urea was certified A.C.S. (Fisher Scientific). [^{13}C]Urea was greater than 99% pure, with water as the major trace contaminant (Isotec) and no detectable contaminants by melting point, NMR and mass spectrometer (MSD Isotopes).

Measurement of exchange parameters

In this technique the nuclear spins of the ^{13}C-enriched urea are aligned in the strong permanent magnetic field of the NMR spectrometer. These spins can be re-oriented 180° by the application of a brief intense radio-frequency pulse of appropriate duration. This re-orientation serves as a label which can be easily measured in the NMR spectrometer. Following the rf pulse, the label decays with a characteristic time constant T_1 (called the spin-lattice relaxation time). T_1 for the label inside the red cell is 17 s, which is much longer than the urea exchange time across the cell membrane (about 0.5 s). T_1 for urea in free solution is even longer (69 s). If, however, the impermeable paramagnetic ion Mn^{2+} is placed in the external solution, the label is quenched in less than 1 or 2 ms. It follows that immediately after a rf pulse, both the intra- and extracellular fluids are labelled, but within a millisecond or two, owing to the external Mn^{2+}, the extracellular label disappears. From this point on, the decay of the label measured from the sample is almost completely due to membrane exchange; urea leaving the cell loses its label upon contact with the external solution, while the urea entering the cells is unlabeled. Since Mn^{2+} is uniformly distributed throughout the entire external solution, there is no extracellular unstirred layer. The 17 s relaxation time for the label inside the cell contributes slightly to the measured value of the decay constant. The true membrane exchange time T_{ex} is related to the measured relaxation time T_1 by the following equation:

$$\frac{1}{T_{ex}} = \frac{1}{T_1} - \frac{1}{17} \tag{1}$$

This equation is derived as follows: in the absence of any membrane-exchange the number of intracellular labels, $N_0(t)$, would decay spontaneously with a time constant of 17 s, i.e.,

$$N_0(t) = n_0 \exp\left(\frac{-t}{17}\right) \tag{2}$$

where n_0 is the total number of spins labeled at time $t = 0$. However, the actual membrane-exchange process

occurring with time constant T_{ex} is superimposed on this slow, spontaneous decay. $N(t)$, the total number of intracellular spins measured at time t is

$$N(t) = N_0(t)\exp\left(\frac{-t}{T_{ex}}\right) = n_0\exp\left(-\left(\frac{1}{T_{ex}}+\frac{1}{17}\right)t\right) \quad (3)$$

By definition of T_1 we have

$$N(t) = n_0\exp\left(\frac{-t}{T_1}\right) \quad (4)$$

Comparison of Eqns. 3 and 4 yields Eqn. 1.

Time constants, T_1, were measured for various urea concentrations at different temperatures using inversion recovery (π–delay–$\pi/2$–acquire). T_1 was also measured for urea in the packed pellet without any external Mn^{2+} quencher to give the decay time (17 s) of the intracellular label. No proton decoupling was necessary due to the molecular structure of the urea molecule.

The urea permeability P_{urea}, is readily calculated from the exchange time T_{ex}

$$P_{urea} = \left(\frac{V}{A}\right)\frac{1}{T_{ex}} \quad (5)$$

where (V/A) is the ratio of cell water volume to membrane surface area. For both a simple carrier or a simple channel, the concentration dependence of P_{urea} can be characterized by two transport parameters (V_{max}, the saturated, maximal transport rate and $K_{1/2}$, the urea concentration required for half saturation as

$$P_{urea} = \frac{V_{max}}{K_{1/2}+C} \quad (6)$$

Results

The diffusional permeability of [^{13}C]urea as a function of concentration and temperature was studied using the inversion recovery technique. Figs. 1 and 2 illustrate raw data obtained by plotting the NMR peak height intensity versus time. The peak height intensity is directly proportional to the amount of labeled [^{13}C]urea inside the cells at any time as given by Equation 4. This experiment, performed at room temperature in 100 mM urea, yields a T_1 of 290 ms (T_{ex} = 295 ms). The figure also shows results for cells treated with 0.05 mM PCMBS, which yield a T_1 of 5.48 s (T_{ex} = 8.08 s). Since urea permeability is inversely proportional to T_{ex} (Eqn. 5) these results translate into a 27-fold decrease in urea permeability at 0.05 mM PCMBS.

Fig. 3 shows the inverse urea permeability, $1/P_{urea}$, at room temperature as a function of urea concentration, C. $1/P_{urea}$ vs. C is linear, a result that is expected if urea moves by either simple channel or simple carrier [12]. From Fig. 3 we recover values for $V_{max} = 1.14\cdot10^{-7}$ mol · cm^{-2} · s^{-1} and $K_{1/2}$ = 680 mM.

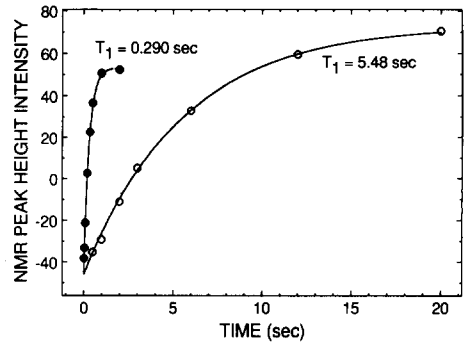

Fig. 1. The solid circles are data acquired for the self-exchange of [^{13}C]urea through the untreated red cell membrane using the NMR inversion recovery technique on a Bruker AM300. Using the exponential T_1 fitting routine supplied by Bruker gives a time constant T_1 = 0.290 s (T_{ex} = 0.295 s). T_1 is related to the exchange time T_{ex} by Eqn. 1 in text. The open circles are data for the self-exchange of [^{13}C]urea through the red cell membrane after being treated with 0.05 mM PCMBS. The T_1 fitting routine gives a time constant T_1 of 5.48 s (T_{ex} = 8.08 s) demonstrating significant inhibition of urea transport.

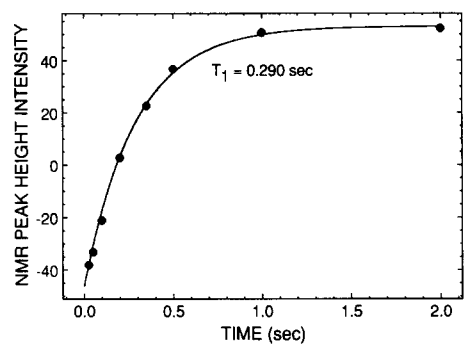

Fig. 2. The solid circles are the data for the untreated cells shown in Fig. 1. The time axis has been expanded for easier viewing of the control.

The temperature dependence of P_{urea} is examined in Fig. 4 which shows an Arrhenius plot of ln P_{urea} vs. $1/T$ for urea concentrations of 100, 200, 500 and 1000 mM. Anomalous behavior is revealed by change in slope as a function of temperature at all concentrations.

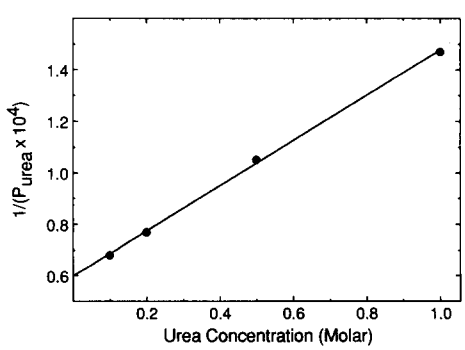

Fig. 3. Hanes-Woolf plot of inverse urea permeability versus urea concentration at room temperature (294 K). From the inverse slope we find $V_{max} = 1.14\cdot10^{-7}$ mol·cm^{-2}·s^{-1} and the intercept/slope gives $K_{1/2}$ = 680 mM.

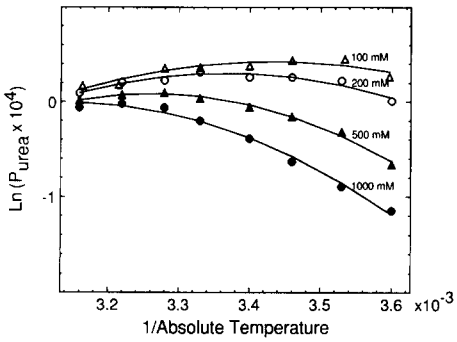

Fig. 4. Arrhenius plot of the natural logarithm of the urea permeability versus the inverse absolute temperature for urea concentrations of 100, 200, 500 and 1000 mM. Unlike the usual Arrhenius plots which yield straight lines for simple physical processes, these smoothly varying curves yield a range of activation energies. At higher temperatures the activation energies appear negative and at lower temperatures positive. At any given temperature the apparent activation energy varies with concentration. The experimental data are fit to theory (solid lines) by plotting the natural logarithm of Eqn. 9 for each urea concentration.

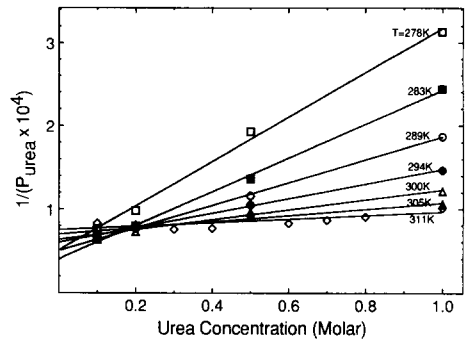

Fig. 5. Hanes-Woolf plot of inverse urea permeability versus urea concentration at seven of eight temperatures studied. The $T = 316$ K curve was left off the figure for clarity of viewing. It would be parallel to and slightly above the curve for $T = 311$ K. The curve for $T = 311$ K was determined at nine different concentrations to allow accurate comparison with Brahm's data [1]. The slope of each curve yields $1/V_{max}$ for that curve, the intercept yields $1/P_0$, and the intercept/slope gives the $K_{1/2}$.

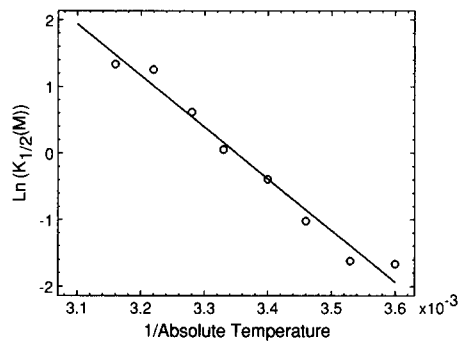

Fig. 6. Arrhenius plot of the natural logarithm of $K_{1/2}$ versus the inverse absolute temperature obtained from the data in Fig. 4. $\Delta H° = 15.5$ kcal·mol^{-1}, $\Delta S° = 51.8$ cal·mol^{-1}·deg^{-1}.

The point of inflection depends on concentration; the maximum occurring at higher temperatures for higher concentrations. This leads to the appearance of a range of activation energies: (1) in any given temperature region for different urea concentrations and (2) at any given concentration for different temperatures. Inflections also have been reported for the transport of Cl^-, Br^- [7] and SO_4^{2-} [13].

For urea, Galey et al. [10] found an activation energy of 11 kcal/mol at a concentration around 750 mM in the temperature range 20 to 30 °C (evaluated from three points). Our data in the same temperature range yield an activation energy of 2.4 kcal/mol at 500 mM urea and 5.3 kcal/mol at 1000 mM urea. Interpolation at 750 mM urea gives an activation energy of 3.8 kcal/mol, significantly lower than reported by Galey et al. Over the temperature range 3 to 38 °C, Brahm [1] found an activation energy of 8.1 kcal/mol for 1 M urea evaluated from five points. Using our average data for those same conditions (seven points with a forced linear fit), we find an activation energy of 6.4 kcal/mol in closer agreement with Brahm.

The apparently anomalous temperature behavior for urea transport can be resolved by taking into account the temperature-dependencies of the individual parameters. Fig. 5 is a family of experimental curves plotted in accordance with Eqn. 6 for 7 of the 8 temperatures studied for ease of viewing. The curve for the highest temperature, $T = 316$ K, is almost horizontal and runs parallel and slightly above the curve for $T = 311$ K and visually obscures the detail, so it was left off the figure. Values of $K_{1/2}$ and V_{max} were obtained from each curve (including $T = 316$ K) and their natural logarithms are plotted as a function of inverse temperature in Figs. 6 and 7 respectively, where the anomalous behavior seen in Fig. 4 has been resolved into two linear well-behaved functions. These can be represented as

$$K_{1/2}(T) = K_{1/2,294} \exp\left[\frac{-\Delta E_K}{R}\left(\frac{1}{T} - \frac{1}{294}\right)\right] \quad (7)$$

$$V_{max}(T) = V_{max,294} \exp\left[\frac{-\Delta E_v}{R}\left(\frac{1}{T} - \frac{1}{294}\right)\right] \quad (8)$$

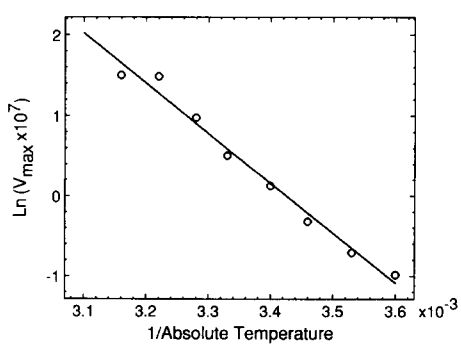

Fig. 7. Arrhenius plot of the natural logarithm of V_{max} versus the inverse absolute temperature obtained from the data in Fig. 4. An activation energy of 12.4 kcal·mol^{-1} is obtained. This value results from a composite of several elementary rate constants (see Eqn.s 13, 20 and 21).

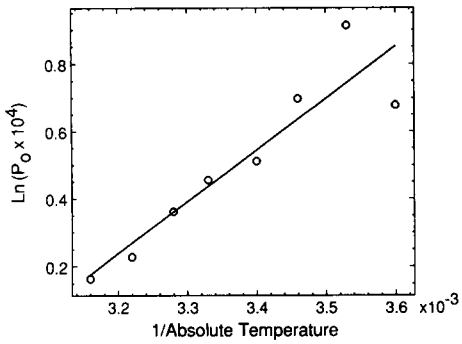

Fig. 8. Arrhenius plot of the natural logarithm of the urea permeability at zero urea concentration (P_0) versus the inverse absolute temperature. A negative activation energy of -3.0 kcal·mol^{-1} is obtained which probably results from the fact that P_0 is a composite of several elementary rate constants (see Discussion, Eqns. 15 and 19).

where $\Delta E_K = 15.5$ kcal/mol and $\Delta E_v = 12.4$ kcal/mol are the apparent activation energies obtained from the slopes of the straight lines in the figures, and $K_{1/2,294} = 0.68$ M and $V_{max,294} = 1.14 \cdot 10^{-7}$ mol · cm^{-2} s^{-1} are the values of $K_{1/2}$ and V_{max} at an arbitrary reference point of 294 K.

The temperature-dependence of urea permeability can be introduced into Eqn. 6 in a straightforward way as

$$P_{urea}(C,T) = \frac{V_{max,294} \exp\left[\frac{-\Delta E_v}{R}\left(\frac{1}{T} - \frac{1}{294}\right)\right]}{K_{1/2,294} \exp\left[\frac{-\Delta E_K}{R}\left(\frac{1}{T} - \frac{1}{294}\right)\right] + C} \quad (9)$$

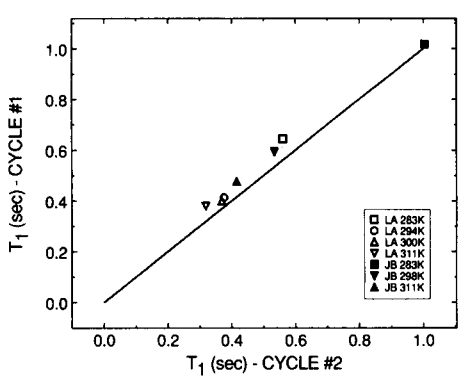

Fig. 9. This figure demonstrates the effect of Mn^{2+} leakage into red cells. After introduction to Mn^{2+} (donor LA – open figures) the cells were subjected to the temperature cycle 1 (283 K – 294 K – 300 K – 311 K) of 78 min duration with equilibration and T_1 measured at each temperature. After a 25 min incubation at 311 K, cycle 2 (311 K – 300 K – 294 K – 283 K) was completed at 170 min. In the second experiment (donor JB – solid figures) Cycle 1 (283 K – 300 K – 311 K) ended 60 min after the initial introduction of Mn^{2+}. Cycle 2 (283 K – 300 K – 311 K) began at 90 min and was complete at 140 min. If the exchange times for cycles 1 and 2 were identical, all experimental points would lie on the straight line of unit slope shown in the figure. The slight deviation from the line indicates a probable Mn^{2+} leakage during twice the length of time required to obtain the temperature data used in this paper. Even for this prolonged time the deviation is insignificant compared to the variations seen with temperature and concentration.

Eqn. 9 is plotted as a continuous curve for reach urea concentration in Fig. 4. It is clear from the figure that this expression, which follows directly from a simple temperature-dependence of the two parameters $K_{1/2}$, and V_{max}, agrees very well with the entire data set.

Fig. 8 is an Arrhenius plot of ln P_0 vs. $1/T$ where P_0 is the urea permeability at zero urea concentration and is seen from Eqn. 6 to equal $V_{max}/K_{1/2}$. A negative activation energy of -3.0 kcal/mol is obtained which probably results from the fact that P_0 is a composite of several elementary rate constants (see Discussion).

The validity of these results requires that no appreciable Mn^{2+} enters the cells during measurements. Recently, Benga [14] reported a decrease in NMR exchange times for water in red cells after they had been exposed to Mn^{2+} for longer than 30 min at temperatures above 20 °C. To evaluate this effect in our experiments on urea transport, we performed the cyclical control experiments summarized in Fig. 9. The effect does not appear to be sufficiently large to affect our results.

Discussion

The principle results of this paper establish the feasibility of using NMR to study [^{13}C]urea exchange, in particular its concentration- and temperature-dependence. Figs. 1 and 2 simply demonstrate the effectiveness of the NMR technique for obtaining time constants for self-exchange flux experiments. Here, a small amount of the known inhibitor of urea transport, PCMBS, is seen to increase the measured decay time constant by almost a factor of 20, which when corrected for spontaneous decay of label translates into a 27-fold increase in the actual membrane exchange time.

Room temperature

Our room temperature estimate $V_{max} = 1.14 \cdot 10^{-7}$ mol · cm^{-2} · s^{-1} compares reasonably well with the value $0.8 \cdot 10^{-7}$ mol · cm^{-2} · s^{-1} reported by Brahm at 25 °C [1], $(1.8 \text{ to } 4.1) \cdot 10^{-7}$ mol · cm^{-2} · s^{-1} by Yousef and Macey [15] and $2.5 \cdot 10^{-7}$ mol · cm^{-2} · s^{-1} by Mayrand and Levitt [2]. Data in Fig. 3 yield a value for $K_{1/2} = 680$ mM which agrees almost precisely with the value (685 mM) obtained earlier with an independent light-scattering method [15]. However, it is higher than other reports of $K_{1/2}$: 218 mM by Mayrand and Levitt and 320 mM by Brahm. This discrepancy in $K_{1/2}$ is reflected when we examine the limiting permeability $P_0 = V_{max}/K_{1/2}$ which occurs as C approaches 0. We obtain $1.67 \cdot 10^{-4}$ cm · s^{-1} as compared to $2.3 \cdot 10^{-4}$ cm · s^{-1} [16], $(2.6 \text{ to } 5.9) \cdot 10^{-4}$ cm · s^{-1} [15], $(2.67 \text{ to } 5.9) \cdot 10^{-4}$ cm · s^{-1} at 25 °C [1] and $11.6 \cdot 10^{-4}$ cm · s^{-1} at 22 to 26 °C [2].

Temperature-dependence

Turning to results on temperature-dependence, our V_{max}, showed a 12-fold increase over the temperature

range 5°C to 43°C, from $0.375 \cdot 10^{-7}$ to $4.512 \cdot 10^{-7}$ mol · cm^{-2} · s^{-1}. This sensitivity to temperature is more substantial than similar measurements reported by Brahm [1] where V_{max} ranged from $0.82 \cdot 10^{-7}$ mol · cm^{-2} · s^{-1} to $1.3 \cdot 10^{-7}$ mol · cm^{-2} · s^{-1} over the temperature range 25°C to 38°C. We also find a 20-fold increase in the value of $K_{1/2}$ from 0.190 M to 3.826 M over the temperature range 5°C to 43°C while Brahm's measurements show that $K_{1/2}$ changes only from 334 to 396 mM between 25°C and 38°C, [1] (our $K_{1/2}$ increases from 1.01 to 3.53 M in the same temperature range). To compare our results with Brahm's at 38°C (311 K), we studied the urea permeability at nine different concentrations (see bottom curve on Fig. 5) using the same donor on two separate occasions. At 38°C we found $K_{1/2} = 3.53$ M and $V_{max} = 4.96 \cdot 10^{-7}$ mol · cm^{-2} · s^{-1} compared to 0.396 M and $1.3 \cdot 10^{-7}$ mol · cm^{-2} · s^{-1} found by Brahm. There is no ready explanation for the differences found in the present study and that of Brahm except in the experimental methods used.

Simple channel with single binding site

Up to this point the discussion is consistent with either a simple channel model with one binding site or with a carrier. Evidence favoring the simple channel model has been presented by Yousef and Macey [15]; and we base our remaining discussion on this assumption. The simple channel model can be represented by the following formal kinetic scheme. If Y represents the concentration of unoccupied membrane sites and CY the concentration of permeant at the site, then the transport process can be represented as

$$C_0 + Y \underset{k_{-1}}{\overset{k_{+1}}{\rightleftharpoons}} CY \underset{k_{-2}}{\overset{k_{+2}}{\rightleftharpoons}} C_{in} + Y \tag{10}$$

where C_0 and C_{in} are the permeant concentrations on the outside and inside of the cell. The unidirectional efflux for a given non-electrolyte will be given by (see Equation 119 in Ref. 12).

$$J_{efflux} = \frac{Y_T k_1 k_2 C_{in}}{(k_{-1} + k_2) + K_1 C_0 + k_{-2} C_{in}} \tag{11}$$

where $Y_T = Y + CY$ represents the total number of binding sites (unoccupied + occupied). Equilibrium exchange efflux J_{exch} occurs when $C_0 = C_{in} = C$,

$$J_{exch} = \frac{Y_T \frac{k_1 k_2}{k_1 + k_{-2}} C}{\frac{k_{-1} + k_2}{k_1 + k_{-2}} + C} \tag{12}$$

Defining the urea exchange permeability $P_{urea} = J_{exch}/C$ and comparing Eqns. 12 and 6,

$$V_{max} = Y_T \frac{k_1 k_2}{k_1 + k_{-2}} \tag{13}$$

and

$$K_{1/2} = \frac{k_{-1} + k_2}{k_1 + k_{-2}} \tag{14}$$

Further, P_0, the maximal permeability that occurs as C approaches zero, is given by

$$P_0 = \frac{V_{max}}{K_{1/2}} = Y_T \frac{k_1 k_2}{k_{-1} + k_2} \tag{15}$$

Finally, applying the equilibrium condition $C_0 = C_{in}$ to Eqn. 10 (see Equation 108 in Ref. 12), we have:

$$k_1 k_2 = k_{-1} k_{-2} \tag{16}$$

Using this relation in Eqn. 14, we see that

$$K_{1/2} = \frac{k_{-1}}{k_1} = \frac{k_2}{k_{-2}} = K_{equil} \tag{17}$$

i.e., $K_{1/2}$ equals the actual equilibrium dissociation constant for the membrane binding site. This allows a relatively straightforward interpretation of the temperature-dependence of $K_{1/2}$. From the slope and intercept of Fig. 6, we obtain an estimate of $\Delta H° = 15.5$ kcal · mol^{-1} and $\Delta S° = 51.8$ cal · mol^{-1} · deg^{-1}. This indicates an entropically driven dissociation. Large entropy changes associated with biological reactions are often explained by the release of hindered or bound water. If we apply this interpretation here, we conclude that release of water occurs when the urea dissociates from the membrane. If so, the more common notion that urea dehydrates upon entering the membrane (association) would not be supported by the data.

It is interesting that both P_0 and V_{max} also give linear Arrhenius plots (see Figs. 7 and 8). Any detailed interpretation of these linearities seems premature, since both parameters are composites of elementary rate constants (see Eqns. 13 and 15). On the other hand, some remarks are appropriate to establish the plausibility of these results. The primary temperature-dependence of each rate constant is proportional to $\exp(-\Delta E/RT)$; let

$$k_i = k_{0i} \exp\left(\frac{-\Delta E_i}{RT}\right) \tag{18}$$

where k_{0i} is a proportionality constant. For P_0

$$P_0 = Y_T \frac{k_1 k_2}{k_{-1} + k_2} = Y_T \frac{k_{01} k_{02} \exp\left(\frac{-(\Delta E_1 + \Delta E_2)}{RT}\right)}{k_{0-1} \exp\left(\frac{-\Delta E_{-1}}{RT}\right) + k_{02} \exp\left(\frac{-\Delta E_2}{RT}\right)} \tag{19}$$

The most apparent way to obtain a linear Arrhenius plot from Eqn. 19 is to assume that $\Delta E_{-1} = \Delta E_2$, or to

to make one of the terms in the denominator sufficiently large so that the other term can be ignored. If we set $\Delta E_{-1} = \Delta E_2$, or if we assume the second term in the denominator is much larger than the first, then in either case the temperature-dependent term in Eqn. 19 will reduce to $\exp(-\Delta E_1/RT)$. Since $\Delta E > 0$ for a single rate constant, this implies that the slope of the Arrhenius plot will be negative which is contrary to the results shown in Fig. 8. The remaining alternative is to assume the first term in the denominator is much larger than the second ($k_{-1} \gg k_2$). Then the temperature-dependent term reduces to $\exp(-(\Delta E_1 + \Delta E_2 - \Delta E_{-1})/RT)$, and a positive slope for the Arrhenius plot will follow if $\Delta E_{-1} > \Delta E_1 + \Delta E_2$.

The same assumption ($k_{-1} \gg k_2$) also predicts the negative slope for the Arrhenius plot of V_{max}. This can be seen if Eqn. 16 is used to eliminate k_{-2} in Eqn. 13, with the result that

$$V_{max} = Y_T \frac{k_{-1}k_2}{k_{-1}+k_2} = Y_T \frac{k_{0-1}k_{02} \exp\left(\frac{-(\Delta E_{-1}+\Delta E_2)}{RT}\right)}{k_{0-1}\exp\left(\frac{-\Delta E_{-1}}{RT}\right) + k_{02}\exp\left(\frac{-\Delta E_2}{RT}\right)} \tag{20}$$

When $k_{-1} \gg k_2$, then

$$V_{max} = Y_T k_{02} \exp\left(\frac{-\Delta E_2}{RT}\right) \tag{21}$$

which yields a negative slope for the Arrhenius plot as observed.

If we pursue the assumption that $k_{-1} \gg k_2$, then $\Delta E_2 = \Delta E_v = 12.4$ kcal/mol as determined from the slope of Fig. 7.

Acknowledgements

We would like to thank Jesper Brahm for his blood and his critical suggestions. This work was supported by NIH: GM18819, NIH: HL37593 and NIH: HL20985.

References

1 Brahm, J. (1983) J. Gen. Physiol. 82, 1–23.
2 Mayrand, R.R. and Levitt, D.G. (1983) J. Gen. Physiol. 81, 221–237.
3 Lippe, C. (1969) J. Mol. Biol 39, 669–672.
4 Vreeman, H.J. (1966) Kon. Ned. Acad. Wet. Ser. B 69, 565–577.
5 Finkelstein, A. (1976) J. Gen. Physiol. 68, 127–135.
6 Poznansky, M., Tong, S., White, P.C. Milgram J.M. and Solomon, A.K. (1976) J. Gen. Physiol. 67, 45–66.
7 Brahm, J. (1977) J. Gen. Physiol. 70, 283–306.
8 Macey, R.I. and Yousef, L.W. (1988) Am. J. Physiol. 254, C699–C674.
9 May, A. and Huehns, E.R. (1975) Br. J. Haematol. 30, 21–29.
10 Galey, W.R., Owen, J.D. and Solomon, A.K. (1973) J. Gen. Physiol. 61, 727–746.
11 Conlon, T. and Outhred, R. (1972) Biochim. Biophys. Acta 288, 354–361.
12 Macey, R.I. (1986) in Physiology of Membrane Disorders (Andreoli, T.E., Hoffman, J.F., Fanestil, D.D. and Schultz, S.G., eds.) pp. 111–131, Plenum, New York.
13 Glibowicka, M., Winckler, B., Aranibar, N., Schuster, M., Hanssum, H., Ruterjans, H. and Passow, H. (1988) Biochim. Biophys. Acta 946, 345–358.
14 Benga, G. (1988) Prog. Biophys. Mol. Biol. 51, 193–245.
15 Yousef, L.W. and Macey, R.I. (1989) Biochim. Biophys. Acta 984, 281–288.
16 Savitz, D. and Solomon, A.K. (1971) J. Gen. Physiol. 58, 259–266.